Colloid Polym Sci (2008) 286:149–157
DOI 10.1007/s00396-007-1771-0

ORIGINAL CONTRIBUTION

AUC and HDC characterization of heterogeneous polymer dispersions

Wendel Wohlleben · M. D. Lechner

Received: 23 April 2007 / Revised: 22 August 2007 / Accepted: 28 August 2007 / Published online: 26 September 2007

Abstract Particle size distributions with high statistical relevance can be assessed by analytical ultracentrifugation (AUC) and hydrodynamic chromatography (HDC) that are based on fractionation. In this paper, we highlight that these techniques are complementary, showcase failures for spherical colloids that are heterogeneous in diameter and density and report remedies. The AUC with well-known turbidity optics measures particle size distributions in the diameter range 20–3000 nm for typical aqueous polymer dispersions. We report the high-resolution evaluation of AUC turbidity time-scan data, with consistent interdependence of diameter, chemical composition, Mie scattering and concentration. For validation, we retrieve correct diameters and shares in mixtures of known components. The method is then applied to a multimodal adhesive raw product. We find drastic effects on relative shares of components. Finally, we confirm the retrieved diameters with the density-insensitive HDC. This commercial apparatus features moderate fractionation power, short measurement times, high repeatability and <3% accuracy on diameters (20–1200 nm), but the obtained shares are misleading in heterogeneous samples.

This manuscript is part of the proceedings of the 16th Symposium Analytical Ultracentrifugation, Hannover, 1st and 2nd March 2007.

W. Wohlleben (✉)
Polymer Physics Research, BASF Aktiengesellschaft,
67056 Ludwigshafen, Germany
e-mail: wendel.wohlleben@basf.com

M. D. Lechner
Physical Chemistry, Universität Osnabrück,
Barbarastrasse 7,
49069 Osnabrück, Germany

Keywords Analytical ultracentrifugation · Hydrodynamic chromatography · Particle size distribution · Density distribution · Mie correction

Introduction

The majority of industrial nanoparticle or colloidal products and polymer dispersion products are formulations of several components that serve different application purposes, and hence, are chemically different. Scientific applications often concern not only nanoparticles with different sizes but also those with different densities [1]. Their characterisation necessitates high statistics and fractionation according to their size or density. Imaging techniques, such as electron microscopy, cannot routinely integrate over more than a few hundreds or thousands of particles; hence, statistics are low. Scattering techniques, such as Fraunhoffer diffraction or dynamic light scattering, evaluate an integrated signal of all fractions and often fail to resolve polydispersity. Both analytical ultracentrifugation (AUC) and hydrodynamic chromatography (HDC) are fractionating techniques that analyse in a single run 20 μl of a suspension at concentration ~1 g/l, corresponding to 10^9–10^{12} particles, depending on their diameter. However, the principles of operation of AUC and HDC induce failures with mixed samples that are heterogeneous in diameter and density. In this paper, we showcase these universal failures and their remedies, and we highlight the complementarity of the two techniques.

Using an AUC equipped with the well-known turbidity optics in time-scan mode can be used to measure better-than-2%-resolution particle size distributions (typically 20–3,000 nm for aqueous polymer dispersions) [2] (Wohlleben et al., submitted). It is obvious that the sedimentation speed

depends on the density difference between solute and solvent. The density-variation method in AUC compares sedimentation coefficients s in chemically identical solvents of different density—such as $s(H_2O)$ vs $s(D_2O)$—and correlates distributions of size and density even in complex mixtures [2, 3].

However, the evaluation can be misleading. To date, the final evaluation from time-scan raw data to an integral multimodal size distribution was done without either high-resolution Mie correction, piecewise or without a constant (average) density. In this paper, we evaluate time-scan turbidity sedimentation measurements with the actual densities for each individual component. The assumptions of this method are: (1) the particles of different densities can be separated by sedimentation, (2) the densities of the particles must be known, and (3) the approximate limiting diameter of the particles with different densities must be known. The evaluation can be performed by applying the classic Stokes' formula together with Mie's theory [4] for each distance from the axis of rotation r (at fixed time t) or for each time t (at fixed distance r).

HDC is complementary to AUC in that the measurement principle of HDC is density-insensitive and relies only on size-exclusion fractionation according to the hydrodynamic diameter of the particles. For standard analyses of size distributions of polymer latices, BASF research and production have replaced AUC by HDC. This commercial apparatus (Fa. Polymer Labs) features moderate fractionation power, but much quicker measurement times, high repeatability and <3% accuracy on sizes and shares.

Due to the density insensitivity, it is much safer than with AUC to determine the diameter fractions in chemically inhomogeneous mixtures. Indeed, HDC confirms the retrieved diameters from the new AUC evaluation algorithm. However, HDC is complementary to AUC also with regard to its failures. Due to its simple UV detection, the shares of fractions are convoluted with the UV activity of the co-monomers of each fraction. This dependence is much stronger than with the $(dn/dc)^2$ dependence of the turbidity detector in AUC. Hence, the determination of shares in chemically heterogeneous samples necessitates our new high-resolution algorithm for the evaluation of AUC turbidity time-scan data.

Theoretical considerations

Nanoparticles are forced in an ultracentrifuge to fractionate according to their size, density and shape. Therefore, it would easily be possible to determine absolutely the whole particle size distribution by detecting the particles as a function of the distance from the axis of rotation r and of the time t. In an AUC, the size determination of infinitely diluted (practically a concentration that is below 1 g/l) spherical colloids is based on *Stokes'* law [5]:

$$d^2 = 18\eta_0 s/(\rho - \rho_0)\ ;\ s = \left(1/\omega^2\right)(d\ln r/dt) \tag{1}$$

with d=diameter of the particle, ρ=density of the particle, s=sedimentation coefficient, η_0=viscosity of the solvent, ρ_0=density of the solvent and ω=angular velocity.

If the particles are detected with absorbance optics, the size distribution (i.e. concentration of each species) can be calculated with *Lambert–Beer*'s law:

$$\ln(I_0/I) = \varepsilon\ C\ l \tag{2}$$

with I_0/I=ratio of the intensities of the solvent and the solution, ε=extinction coefficient, C=concentration of the particles and l=path length.

The extinction coefficient ε may be calculated by *Mie*'s scattering theory [6]. Starting with *Maxwell*'s equations the extinction efficiency Q_{ext} as a function of the size parameter $\pi\ d/\lambda$ (d=diameter, $\lambda=\lambda_0/n_0$=wavelength), the density of the particle ρ and the refractive indices of the solvent n_0 and the particle n_1 has been developed. In the case that the incident light is not only scattered but also absorbed by the particle, the complex refractive index of the particle $N_1 = n_1 + i\ k_1$ with $i=(-1)^{1/2}$ has to be applied. Mie has calculated Q_{ext} for homogeneous isotropic spheres [6]. Different authors have calculated Q_{ext} for inhomogeneous spheres with a refractive index gradient, for coated spheres, for ellipsoids and for cylinders [7].

The relation of the extinction efficiency Q_{ext} and the extinction coefficient ε is given by [7].

$$\varepsilon = 3Q_{ext}/(2dp);\ (\text{sphere with diameter } d) \tag{3}$$

$$\varepsilon = \pi Q_{ext}/(dp);\ (\text{cylinder with diameter } d \text{ and infinite length}) \tag{4}$$

Figures 1 and 2 demonstrate the extinction coefficient ε (sometimes called specific turbidity $\varepsilon=\tau/C$) as a function of the reduced size parameter $\pi\ d/\lambda$ for different ratios n_1/n_0 for spheres. The ε values were calculated according to Mie's theory [6, 7] and according to Eq. 3 with ρ=1 g/cm^3. For densities of the particles which differ from unity, one has to divide the ε values with ρ. The lower diameter scale refers to a wavelength λ_0=546.1 nm and a refractive index of the solvent of n_0=1.333. The rippling of some curves is due to oscillations of the Bessel functions included in Mie's equations. The figures show that Mie's theory includes the *Rayleigh* scattering of small molecules with diameters

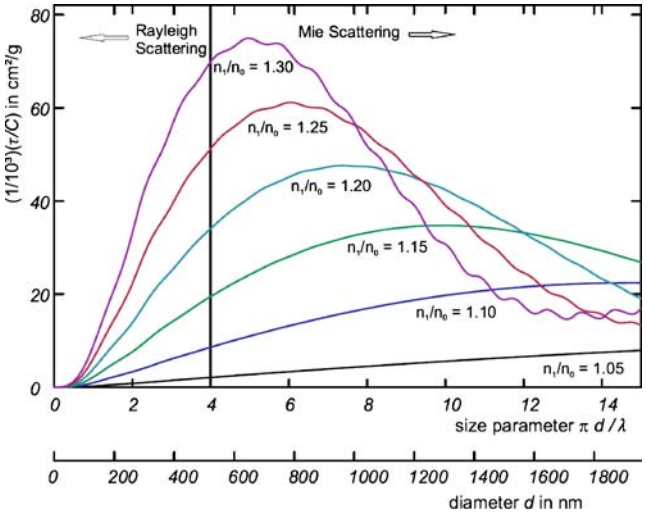

Fig. 1 Colloidal particle scattering: Extinction coefficient $\varepsilon = \tau/C$ for spheres as a function of the size parameter $\pi\ d/\lambda$ for different relations of the refractive indices n_1/n_0 in the region $0<\pi\ d/\lambda<15$; the lower diameter axis refers to λ_0=546.1 nm and n_0=1.333

down to 1 nm. As has been shown by Dezelic and Kratohvil [8], the theories of Rayleigh and Mie are nearly identical with respect to the extinction coefficient in the range $0<\pi\ d/\lambda<0.3$. Figures 1 and 2 indicate the angle independent Rayleigh scattering ($d<\lambda/20$), the angle dependent Rayleigh scattering ($\lambda>d>\lambda/20$) and the Mie scattering ($d>\lambda$).

The calculation of $\varepsilon=\tau/C$ in conjunction with the law of Lambert–Beer, Eq. 2 enables the determination of the concentration of the particles C if the optical density $\ln(I_0/I)$ and the thickness of the solution in a cuvette can be measured. Fractionation of the particles by applying a gravitational or centrifugal field allows the determination of the particle size distribution.

In principle, there are two possibilities for the measurement of the particle size distribution with an analytical ultracentrifuge:

A) The AUC has a variable slit position, moving as fast as possible during distinct times from the meniscus to the cell bottom. A lamp illuminates the slit and a light detector measures the intensity $I(t)$ as a function of the rotor distance r. This method may be improved by positioning many light detectors, i.e. photodiodes along the complete distance from the cell meniscus r_m to the cell bottom r_b.

B) The AUC has a constant slit with a radius position at mid-cell $r_s \approx (r_m+r_b)/2$. A lamp illuminating the position slit together with a light detector measures the intensity $I(t)$ of the moving particles at a constant rotor distance r_s. The following equations hold for this turbidity time-scan method.

Following Eq. 2, the ratio of the turbidity at the time t, $\tau(t)=\varepsilon(t)\ C$ and the turbidity at the time $t=0$, $\tau(0)=\varepsilon(0)\ C$ can be determined via the experimentally accessible intensities of the solution and the solvent:

$$\tau(t)/\tau(0) = \{\ln[I(t)/I_0]\}/\{\ln[I(0)/I_0]\} \tag{5}$$

where $I(t)$ and $I(0)$ are the intensities of the solution at the time t and at the time $t=0$ respectively, and I_0 is the intensity of the solvent. In the case that all dissolved or dispersed particles have identical extinction coefficients $\varepsilon_i=\varepsilon$, the relative concentration of the particles could easily be determined:

$$\tau(t)/\tau(0) = C(t)/C(0) = W(d) \tag{6}$$

Using an analytical ultracentrifuge, particles with different sizes can be fractionated on the basis of their diameter. Using Stokes' well-known equation [5] and the assumption that the bare radius equals the hydrodynamic radius:

$$d_i^2 = 18\eta_0 s_i \Big/ [\rho(r,t)-\rho_0]\ ;\ s_i = [\ln(r_s/r_h)] \Big/ \int \omega^2 dt \tag{7}$$

with d_i=diameter of the species i, η_0=viscosity of the solvent, s_i=sedimentation coefficient of the species i, $\rho(r,t)$=density of the solute at distance r and time t, ρ_0=density of the solvent, r_s=radius position of the slit in the ultracentrifuge cell, $r_h=r_m$=radius position of the meniscus in the cell in the case of sedimentation of the particles, $r_h=r_b$=radius position of the bottom in the cell in the case of flotation of the particles, and ω=angular velocity of the rotor.

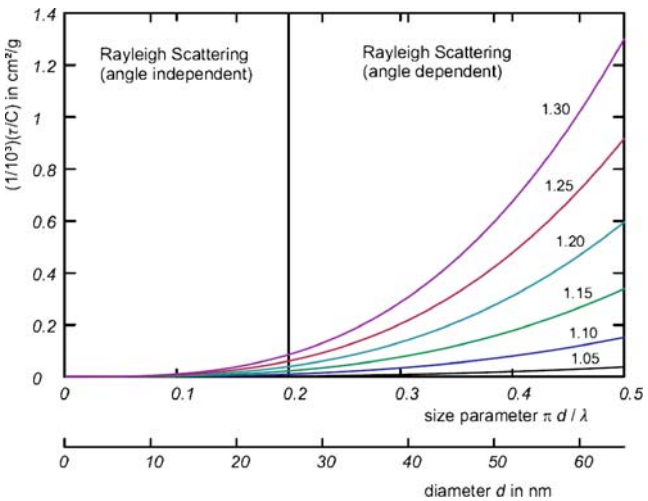

Fig. 2 Nanoparticle scattering: extinction coefficient $\varepsilon=\tau/C$ for spheres as a function of the size parameter $\pi\ d/\lambda$ for different relations of the refractive indices n_1/n_0 in the region $0<\pi\ d/\lambda<0.5$; the lower diameter axis refers to λ_0=546.1 nm and n_0=1.333

For sector shaped cells, the dilution rule has to be applied:

$$C_i(t) \Big/ C_{i,0} = (r_h/r_s)^2 \tag{8}$$

In the case of different particle sizes, one has to apply for each species a different extinction coefficient $\varepsilon_i=(\tau/C)_i$ according to Eqs. 3 and 4:

$$\tau(t)/\tau(0) = \sum_{i=1}^{N} \tau_i(t)/\tau(0)$$

$$= (1/\varepsilon_0) \sum_{i=1}^{N} \varepsilon_i \, C_i(t)/C(0) \tag{9}$$

with i=1, 2,..., N being the species number.

Using a slit with a constant radius position r_s (possibility B), the evaluation procedure is as follows:

Considering the measured turbidity time-scan $I(t)$ curve as a superposition of N $I(t)$ curves for monodisperse particles, the evaluation starts with the smallest particle at the largest possible time with a density $\rho(t)$ [2, 9]. The appropriate diameter d_i of this particle is calculated according to Eq. 7 and the appropriate concentration $C_i(t)$ according to Eqs. 5, 6, 8 and 9. The procedure is then continued by recurrence calculation, proceeding from the smallest to the largest particles using Eqs. 5 to 9 with the appropriate densities of the particles $\rho(t)$. It is a prerequisite that the particles with different densities and different diameters have to be separated by sedimentation; otherwise, this method does not work. In several cases, it would be possible that the particles of different sizes and densities are separated.

Experimental materials and methods

Polymer dispersions

For validation purposes, polymer dispersions are synthesised in surfactant-free emulsion polymerisation [10]. The main

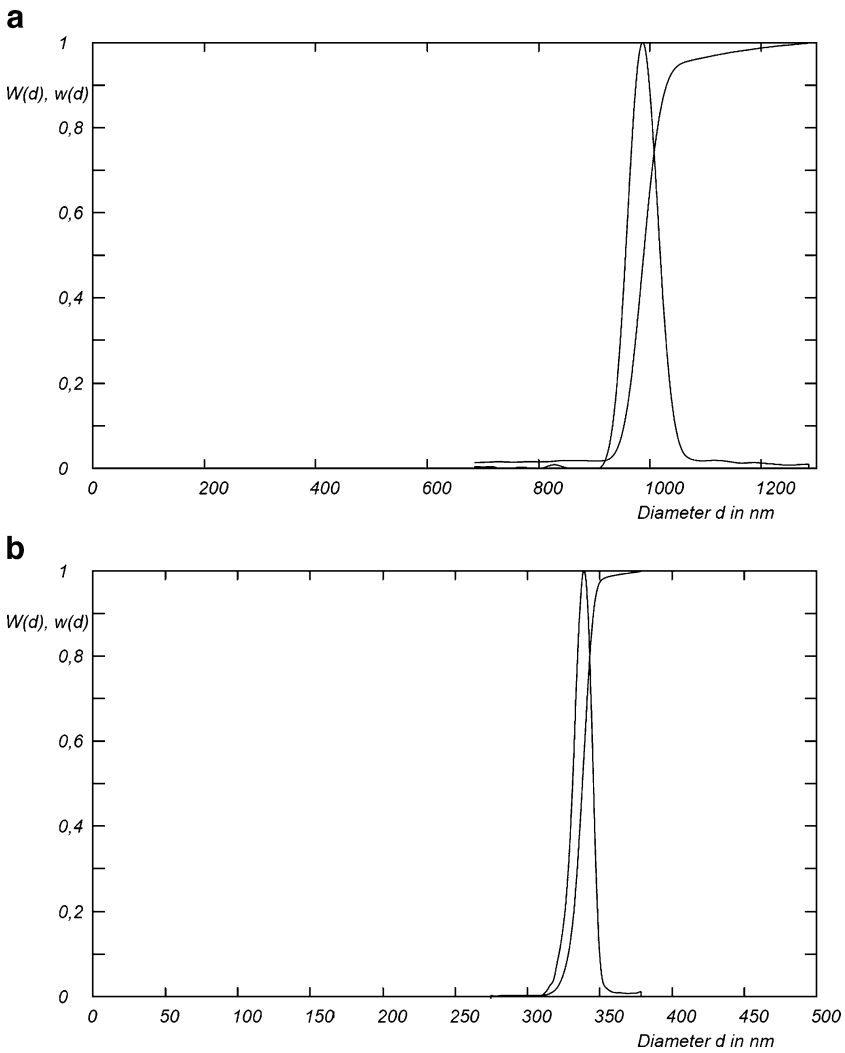

Fig. 3 Integral $W(d)$ and differential $w(d)$ particle size distributions of the test polymer dispersion 1 (*top*) and 2 (*bottom*) measured and evaluated by standard routines of the turbidity time-scan AUC

monomer is styrene, but additional monomers shift the density of the particles to different values: Dispersions 1 and 2 have a density ρ of 1.054 and 1.079 g/cm^3, respectively.

The unknown sample to be characterised by AUC and HDC is an acrylic dispersion from BASF polymer research being developed as adhesive raw product. The dispersion is made to be bimodal to increase the solid content and yet to maintain low viscosity. This procedure exploits the well-known effect that smaller particles replace the water in the interstices between the larger particles—a diameter ratio of small/large=1:5 and shares=25:75 are optimal; therefore, less water is needed to keep the product flowable. Unintentionally, the two fractions have different monomer compositions with different densities.

Turbidity AUC

We use a home-built turbidity optics similar to the one described in [2], with Labview-based electronics and green (wavelength 546 nm) detection light focussed to 0.5 mm at mid-cell. Transmission is recorded with 40 values for each passing-by of the cell under the laser, with 300 passing-bys registered per second per cell. As discussed in "Theoretical considerations" above, the AUC is an absolute technique that requires no calibration.

Hydrodynamic chromatography

Hydrodynamic chromatography is purchased as a 'particle size distribution analyzer' or PSDA™ from Polymer Labs with an integrated autosampler. The fractionation mechanism is size exclusion: The sample is injected into a packed column of solid polysterene beads for which the exact pore size distribution and bead functionalisation are proprietary with the manufacturer. We use 'column 2', with a nominal range of 20–1200 nm. The aqueous elution medium contains salts with anionic and non-ionic surfactants, again of proprietary composition, to minimise interaction between sample and column. Indeed, the column and elution medium has proven to be universal for all anionic latices,

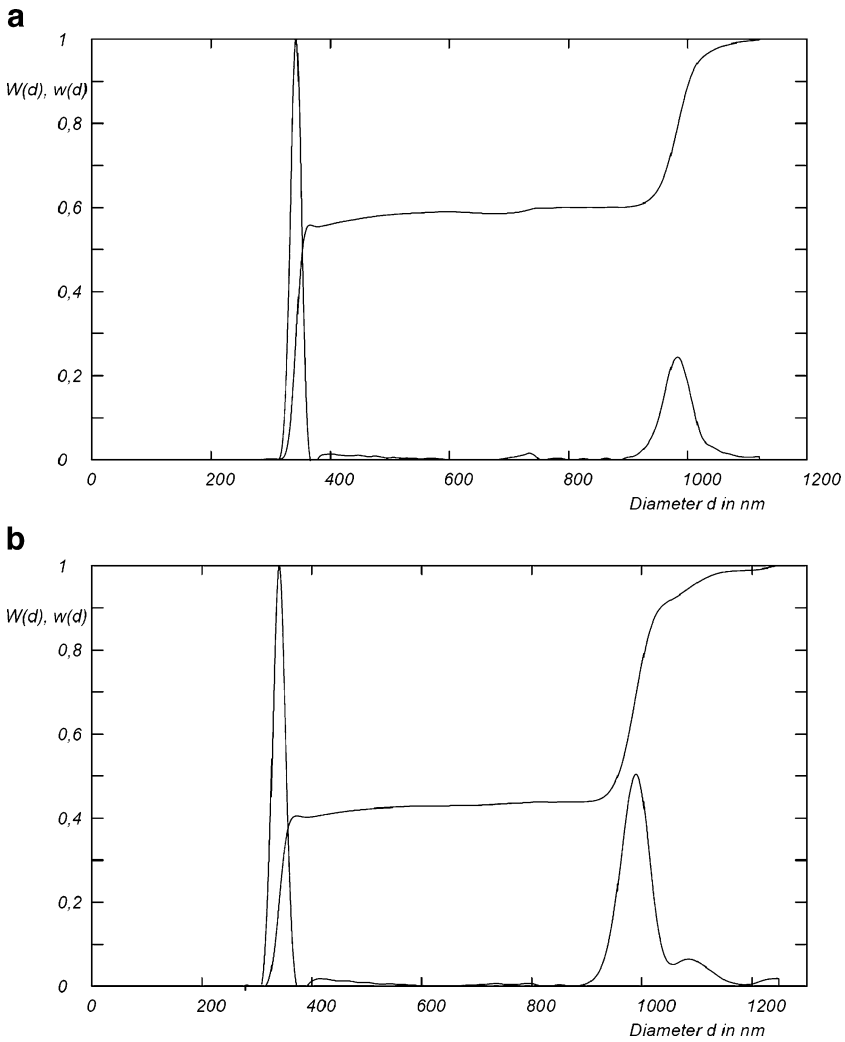

Fig. 4 Validation of the multiple-density AUC evaluation algorithm with a sample of dispersions 1 and 2 in the known mixtures 59/41 (*top*) and 43/57 (*bottom*). The diameters are retrieved with better than 1% deviation, and the shares are retrieved with better than 5% deviation

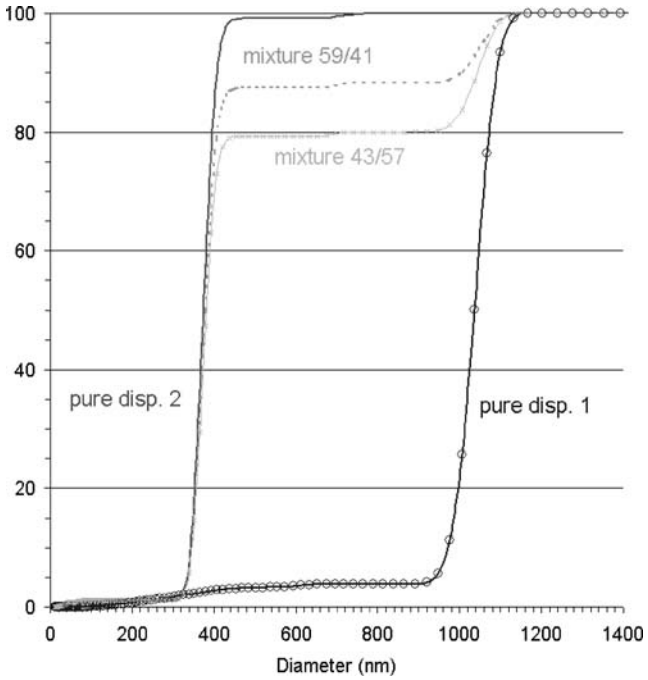

Fig. 5 Validation of the multiple-density evaluation algorithm with HDC measurements of the same samples as in Fig. 4: dispersion 1 (*solid line* with *circles*), dispersion 2 (*solid line*) and the mixtures 59/41 (*dashed line*) and 43/57 (*crosses*). The diameters are retrieved with better than 1% deviation, but the shares are misinterpreted due to the simple UV detection scheme of the commercial apparatus

and we do not tune the HDC in any way for a specific sample. The particles with smaller hydrodynamic diameter diffuse into more interstices, and hence, take longer time to elute from the column. After elution from the column, the particles are detected by the UV absorbance at 254 nm, which is the optimal wavelength to monitor polystyrene. The HDC elution time and elution shape are calibrated with nine standard latices between 20 and 1400 nm; hence, all diameters are only as accurate as the standards, which are specified to 2% accuracy by the manufacturer (Duke).

The raw elution data achieve baseline resolution (meaning that the elution curve returns to zero between two peaks) for a factor 2 between the hydrodynamic diameters of neighboring peaks. This raw-data-resolution cannot compete with turbidity time-scan AUC. However, the HDC software deconvolutes the shape of standard latices, which are assumed to be ideally monodisperse, and are specified with 1% rms deviation in diameter. This assumption is hence valid in all practical applications, as the vast majority of polymer dispersions to be characterised have much larger polydispersity. The resulting accuracy of HDC is better than 3% in diameter and better than 3% on shares of sufficiently separated fractions. Typical elution time is 8 min, and the entire experiment time between sample injection and final size distribution graph is 15 min.

Experimental results

Validation

The particle size distribution of the test dispersions 1 and 2 are shown in Fig. 3. We find mean diameters of 988 and 337 nm, respectively, accounting for the different densities of 1.054 and 1.079 g/cm^3, respectively. We now mix these dispersions in the ratio of 59/41, and with the new multiple-density evaluation of the turbidity time-scan data, we find the size distribution shown in Fig. 4a. Note that we retrieve the correct diameters and reasonably good shares of 340 nm (55 wt%) and 980 nm (45 wt%). The retrieved ratio 55:45 deviates slightly from the actual ratio 59:41, and we ascribe this to the uncertainty in dn/dc values, which influence the

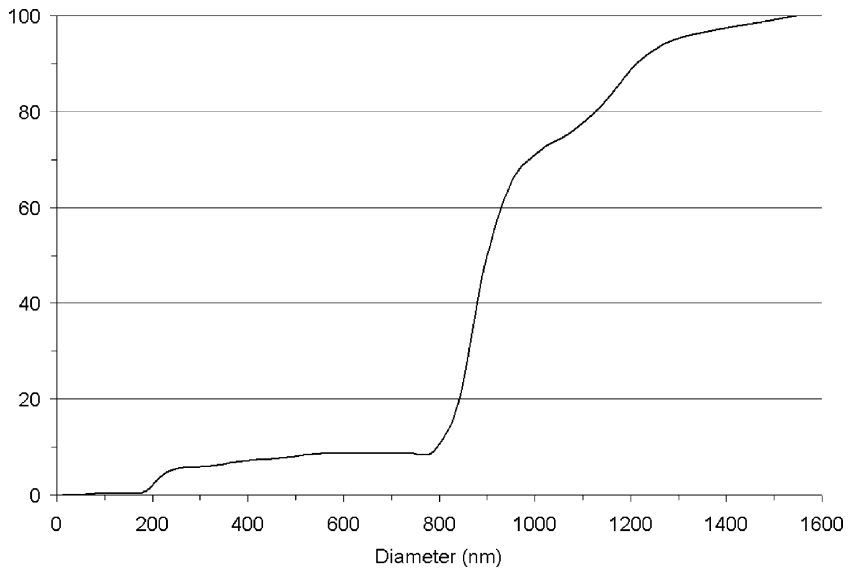

Fig. 6 HDC particle size distribution of the unknown adhesive raw product. The hydrodynamic diameters of the sample are bimodal with main fractions at 200 and 820 nm and a coarse fraction at 1,200 nm

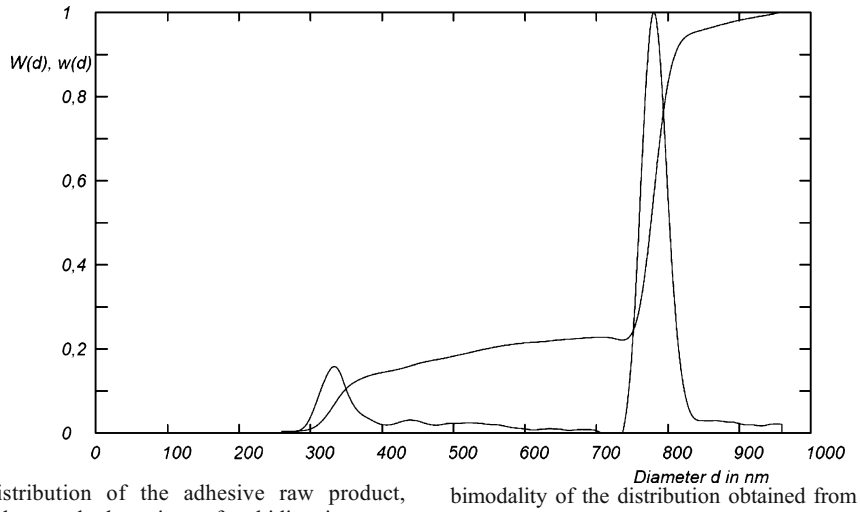

Fig. 7 Particle size distribution of the adhesive raw product, measured and evaluated by standard routines of turbidity time-scan AUC, with the density of the main component of 0.999 g/cm^3. The bimodality of the distribution obtained from HDC data is confirmed, but the diameters strongly deviate from the diameters determined from AUC, which indicates that the assumed particle densities are incorrect

Mie correction. As another test, we mix the same dispersions in the ratio 43:57 (Fig. 4b). Again, the diameters and shares are retrieved correctly. From these two test samples, we estimate that with our new multiple-density evaluation of turbidity AUC time-scan data, the diameters are retrieved with better than 1% deviation, and the shares are retrieved with better than 5% deviation.

In the following, we compare the turbidity AUC time-scan results to results obtained from HDC. The pure polymer dispersions and their mixtures are characterised all at the same conditions for measurement and evaluation without any special attention to their chemical inhomogeneity (Fig. 5). Obviously, the HDC correctly reproduces the diameters irrespective of different densities. However, the shares are largely misinterpreted due to the different UV absorption cross-section of polymer dispersions 1 and 2. In principle, a correction for the UV absorption cross-section is feasible—but in the commercial stand-alone software from Polymer Labs, there is no such option. The important advantages of HDC, i.e. easy determination of diameters in multimodal samples, speed and price, are balanced by the disadvantage of systematic uncertainty in relative shares as soon as the different fractions deviate in chemical composition.

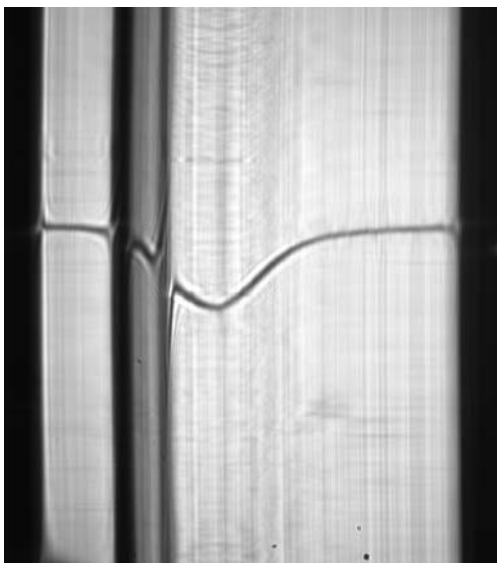

Fig. 8 AUC Schlieren image of a dynamic density gradient 6 min after preparing the layers solvent and solution; adhesive raw product. The *solid line* that connects the dark areas at the *left* (meniscus) and *right* (bottom) reflects the continuous decrease in optical density between H_2O and D_2O. The sample was dissolved at 0.01 mg/ml in D_2O then overlayered by H_2O at 40,000 rpm. The density of the sample is clearly inhomogeneous. The two main turbid peaks correspond to densities of 0.999 and 1.012 g/cm^3

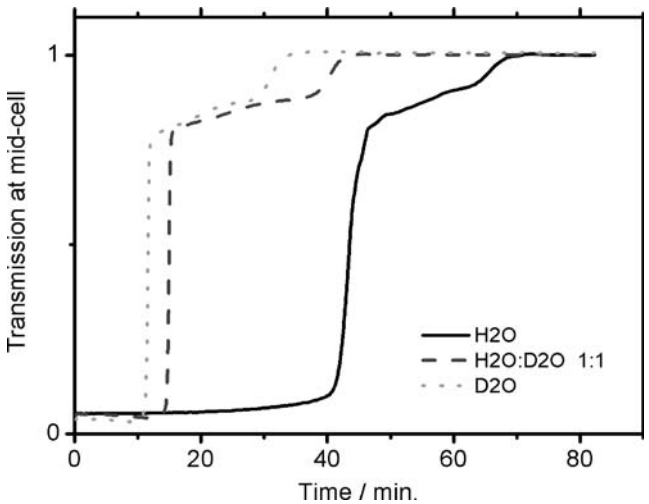

Fig. 9 Raw data of a density variation experiment with the turbidity time-scan AUC. The three turbidity time-scans, scaled to equal turbidity at time zero for evaluation, are brought to accordance with one fraction around 800 nm with density 0.999 g/cm^3 and a second fraction around 200 nm with density 1.004 g/cm^3. The accuracy of the retrieved density for the smaller fraction is affected by the scaling procedure, as the turbidity signal is small and not identical for the different solvents

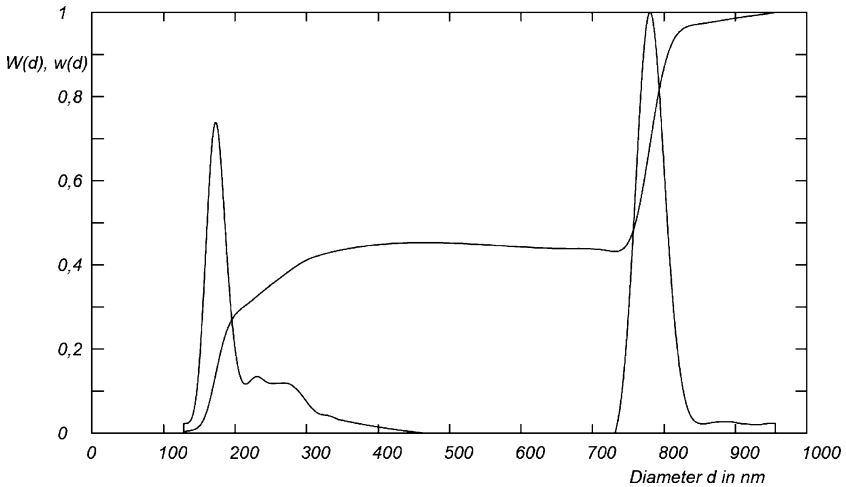

Fig. 10 Multiple-density evaluation of the AUC turbidity time-scan data on the adhesive raw product. The diameters are now in good accordance with the straight-forward density-insensitive measurement by HDC (Fig. 6). The relative share of the smaller particle fraction is drastically higher compared with the naive evaluation (Fig. 7) because of the interdependence of density, diameter and Mie corrections

Application to an unknown sample (adhesive raw product)

As nothing was known about the outcome of this particular synthesis, we started by measuring the hydrodynamic size distribution with HDC (Fig. 6). We find two fractions, centered at 200 and 820 nm, respectively, and a coarse fraction at 1,200 nm. In a naive turbidity AUC time-scan measurement, we use the known density of the larger component for evaluation. The result (Fig. 7) corroborates the bimodality of the sample, but the retrieved diameters of 330 and 800 nm deviate drastically from the hydrodynamic diameters from HDC. The fact that the coarse fraction from HDC is vanishing in the AUC data hints to a much-enhanced UV activity of this fraction. As the diameters depend only on viscosity and density difference, with the viscosity being well known, there must be an inhomogeneity in the densities. For a correct AUC determination of particle sizes, we have to use more elaborate (and time-consuming) methods.

First, we check the density distribution in a dynamic density gradient [2, 11]. The sample is dissolved at 0.01 mg/ml in D_2O then overlayered by H_2O at 40,000 rpm. Every 2 min, we record a Schlieren image [2, 12] of the resulting refractive index distribution. Here, we select the 6-min image for evaluation (Fig. 8). The density of the sample is clearly not homogeneous. The two main peaks are identified at densities of 0.999 and 1.012 g/cm^3.

To correlate the bimodality in density with the bimodality in diameter, we perform a density variation experiment with the turbidity time-scan AUC [2]. The raw data show one fraction that sediments extremely slowly in H_2O, hence, with a density very close to H_2O (Fig. 9). A second fraction with smaller turbidity sediments slower in all solvents, but with a stronger difference between the sedimentation, speeds in D_2O and D_2O/H_2O mixture. Hence, this fraction consists of particles with a smaller diameter and higher density. These hand-waving interpretations are confirmed by the rigorous analysis: The three turbidity time-scans are brought to accordance with one fraction around 800 nm with density 0.999 g/cm^3 and a second fraction around 200 nm with density 1.004 g/cm^3. Concerning the disagreement of absolute density values from density gradient and from density variation, it should be noted that for evaluation of the density variation data, the three curves are scaled to equal turbidity at time zero and at infinite time. The accuracy of the retrieved density for the smaller fraction is affected by the scaling procedure, as the turbidity signal is small and not identical for the different solvents (Fig. 9). In summary, the

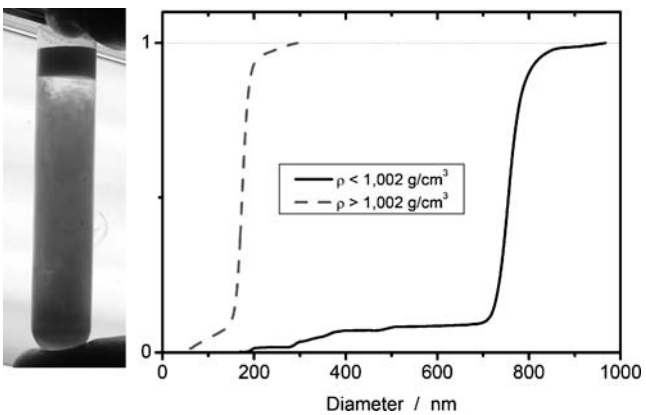

Fig. 11 Preparative fractionation with a water mixture of density 1.002 g/cm^3 at 54,000 rpm for 60 h in the swing-bucket rotor. We successfully obtain one flotate and one sediment fraction. The characterisation of the redispersed fractions confirms that the sediment with density >1.002 g/cm^3 (*dashed line*) consists exclusively of the 200-nm particles and the flotate with density <1.002 g/cm^3 (*solid line*) contains the 800-nm fraction

smaller particles have clearly the higher density, in accord with the weaker turbidity of the higher-density peak in the density gradient (Fig. 8).

We can now evaluate the time-scan turbidity data with the new multiple-density algorithm where we select the density of 0.999 g/cm^3 for the larger particles (above 350 nm) and 1.004 g/cm^3 for the smaller particles. The diameter values in the resulting size distribution (Fig. 10) are now in good accordance with the straight-forward density-insensitive measurement by HDC (Fig. 6). The relative share of the smaller particle fraction is drastically higher compared with the naive evaluation (Fig. 7) because of the interdependence of density, diameter and Mie corrections. We cannot expect an agreement of the relative shares obtained from HDC and AUC and the actual shares because of the inhomogeneous chemical composition. We have good reason to suspect that the larger particles contain more UV-absorbing monomers that induce the overestimation of the share of larger particles in the HDC measurement.

Finally, if all of the above holds, it should be possible to separate the two fractions on the basis of their density. To that end, we mix H_2O and D_2O with a density of 1.002 g/cm^3, i.e. in between the two retrieved densities. The sample is diluted at 11 wt% in this water mixture and then centrifuged at 54,000 rpm in the swing-bucket rotor. After 2 h, phase separation sets in and is complete after 60 h (Fig. 11). We expect to find all components with density <1.002 g/cm^3 in the flotate and all components with density >1.002 g/cm^3 in the sediment. For verification, we redisperse the flotate and the sediment. Indeed, we find that the sediment consists exclusively of the 200-nm fraction and the flotate contains the 800-nm fraction. This measurement also shows that the intermediate sizes of 350–700 nm belong to the low-density fraction.

Summary and conclusion

In heterogeneous colloid samples, the diameter of each fraction is reliably determined from HDC, but the fractions' shares can be vastly misleading. On the same samples, the evaluation of AUC data requires careful consideration of each fraction's density. Only then are the diameters, and also the shares, correct on the few-percent level.

We have developed, tested and applied a high-resolution algorithm for the evaluation of AUC turbidity time-scan data with consistent interdependence of diameter, chemical composition, Mie scattering and concentration. The assumptions of this method are: (1) the particles of different densities can be separated by sedimentation, (2) the densities of the particles must be known, and (3) the approximate limiting diameter of the particles with different densities must be known. Under these conditions, we consider the measured turbidity time-scan as a superposition of independent monodisperse particles. The evaluation starts with the smallest particle at the largest possible time and continues by recurrence calculation, proceeding from the smallest to the largest particles, with the appropriate densities of each individual fraction.

Applied to an unknown multimodal sample (adhesive raw product), we had to perform time-consuming analyses that involved dynamic density gradient (Schlieren AUC) and density variation experiments (turbidity AUC) to finally confirm the particle diameters from the 15-min straight-forward measurement with the density-insensitive HDC. The important advantages of HDC, i.e. the determination of diameters in multimodal samples, ease and speed of operation and price, are compromised by the systematic uncertainty in relative shares as soon as the different fractions deviate in chemical composition. Here, our new multiple-density AUC method finds drastic effects on relative shares of components. The findings are confirmed by a successful preparative fractionation of the unknown sample according to density.

Future alternatives with a more simple algebraic routine may rely on HDC or ramped-speed AUC with low-concentration refractive index detectors.

Acknowledgements We gratefully acknowledge excellent laboratory support from Manfred Stadler and Kai Werle. We are indebted to the referees for exceptionally careful and constructive comments.

References

1. Cölfen H (2005) In: Scott DJ, Harding SE, Rowe AJ (eds) Analytical ultracentrifugation. Techniques and methods. The Royal Society of Chemistry, Cambridge, pp 501–583
2. Mächtle W, Börger L (2006) Analytical ultracentrifugation of polymers and nanoparticles. Springer, Berlin
3. Müller HG, Herrmann F (1995) Progr Colloid Polym Sci 99: 114–119
4. Lechner MD (2005) J Serb Chem Soc 70:361–369
5. Lechner MD, Mächtle W (1999) Progr Colloid Polym Sci 114: 37–43
6. Mie G (1908) Ann Phys 25:377
7. Bohren CF, Huffman DR (2004) Absorption and scattering of light by small particles. New York, Wiley
8. Dezelic G, Kratohvil JP (1960) Kolloid-Z 173:38
9. Mächtle W (1988) Angew Makromol Chem 162:35–52
10. Reese CE, Asher SA (2002) J Colloid Interface Sci 248:41–46
11. Börger L, Lechner MD (2006) Colloid Polym Sci 284:405–412
12. Börger L, Lechner MD, Stadler M (2004) Progr Colloid Polym Sci 127:19–25